

Cathodic Protection of Bridge Substructures: Burlington Bay Skyway Test Site, Initial Performance of Systems 1 to 4

H. C. SCHELL, D. G. MANNING, and K. C. CLEAR

ABSTRACT

The performance of four experimental cathodic protection systems during the first 8 months of operation is described. The systems were installed on the columns of the Burlington Bay Skyway Bridge in 1982. The method of data collection and the essential features of the performance of each system are described. Macrocells and current pick-up probes were found to be the most useful tools for monitoring cathodic protection systems. The three impressed-current systems were all effective in stopping corrosion. Insufficient power was available from the galvanic system for it to be practical. The durability of some system components needs to be improved. The future work required to develop a full-scale operational cathodic protection system for bridge substructures is discussed.

Four experimental cathodic protection systems were installed on the columns of Burlington Bay Skyway Bridge in 1982. The methods of data collection and analysis and the performance of the systems during the first 8 months of operation are described.

DESCRIPTION OF SYSTEMS AND INSTRUMENTATION

Although the four systems have been described in detail elsewhere (see paper by Manning et al. elsewhere in this Record), the salient features of each are repeated for reference purposes. Systems 1, 2, and 3 were powered by impressed current, and the primary anode in all cases was a conductive polymer concrete. In System 1 the anodes were used with a shotcrete overcoat. System 2 consisted of the primary anodes with an exposed secondary anode of conductive paint. System 3 employed a secondary anode network of multifilament carbon strand and a shotcrete overcoat. System 4 was a sacrificial anode system that used zinc ribbon anodes and a shotcrete overcoat. Each system was applied to the four faces of a rectangular column and covered approximately 38 m² of concrete area.

The instrumentation that was designed and installed to measure the performance of the cathodic protection systems has also been described elsewhere (see paper by Manning et al.). It consisted of macrocells, current pick-up probes, current distribution probes, and electrical resistance probes. The macrocell is a strong natural corrosion cell in which current flow can be measured. The amount of current that must be applied to reverse the direction of current flow in the macrocells is a measure of the effectiveness of the cathodic protection. A

zinc-zinc sulfate reference cell was embedded in each macrocell. The current pick-up probes were short pieces of rebar embedded at the level of the reinforcing steel at various points in the structure. They are used to measure current density. The current distribution probes consisted of three current pick-up probes installed in a line at different depths from the concrete surface. They are used to measure the variation in current density with depth. The electrical resistance probes were designed to give a quantitative measurement of corrosion in terms of metal loss per year. Figures 1-4 show the number, location, and identification of the instrumentation in the four systems.

The instrumentation and anode leads were terminated in a single junction box for each system. A schematic diagram of a typical box is shown in Figure 5. All the measurements were made at the box. The control panel within each junction box was designed to allow connections to be changed readily, thus allowing maximum flexibility to investigate parameters such as anode spacing.

The three impressed-current systems were each powered by a separate, unfiltered full-wave rectifier that had a maximum output of 16 V and 12 A. The positive terminal of the rectifier was connected to the anode lines and the negative terminal was connected to a ground on the reinforcing steel. This ground connection was not used for any measurements other than rectifier output voltage.

METHOD OF DATA COLLECTION

Current Measurements

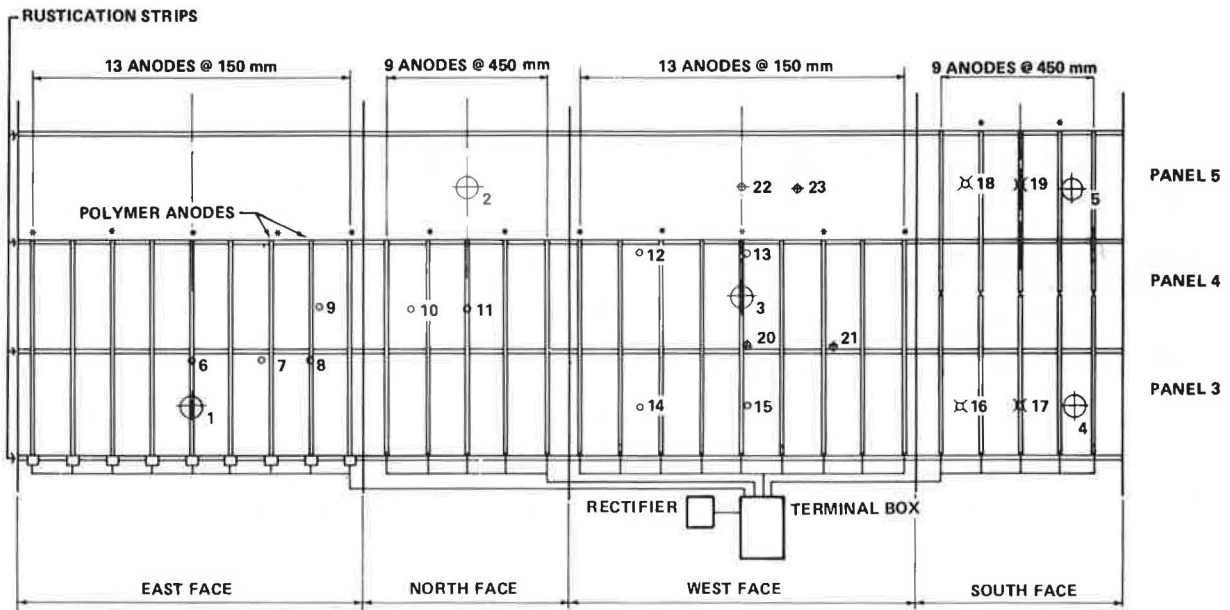
Anode Feeder Lines

The anodes in Systems 2 and 3 were supplied by individual feeder lines. In Systems 1 and 4 the anodes on each face of the column were connected so that a separate anode feeder line supplied all the anodes on one face. These connections are shown in Figures 1-4. A switch was placed in each line. In System 4 the anode feeder lines were connected to a ground on the corresponding face of the column. Current measurements were made by measuring voltage drop across a high wattage resistor placed in each line.

Macrocell Rebar Probes

The leads from the macrocell rebar probes were connected through a resistor to the ground connection within the same macrocell. The resistor size was chosen to be approximately 10 percent of the open circuit alternating current (ac) resistance between the probe and ground. The magnitude and direction of the current flow between the probe and the reinforcing steel was determined by measuring the voltage drop across the resistor.

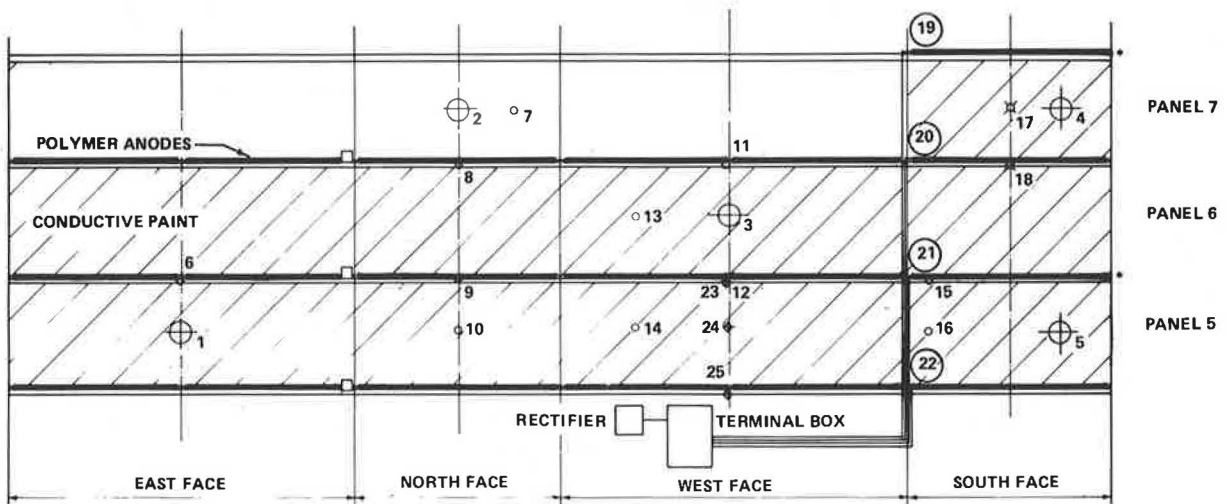
Throughout this study the convention used was to



INSTRUMENTATION	1 – 5	MACROCELLS
	6 – 15	CURRENT PICKUP PROBES
	16 – 19	CURRENT DISTRIBUTION PROBES
	20 – 23	ELECTRICAL RESISTANCE PROBES

* ANODES DISCONNECTED APRIL 13 - JUNE 14

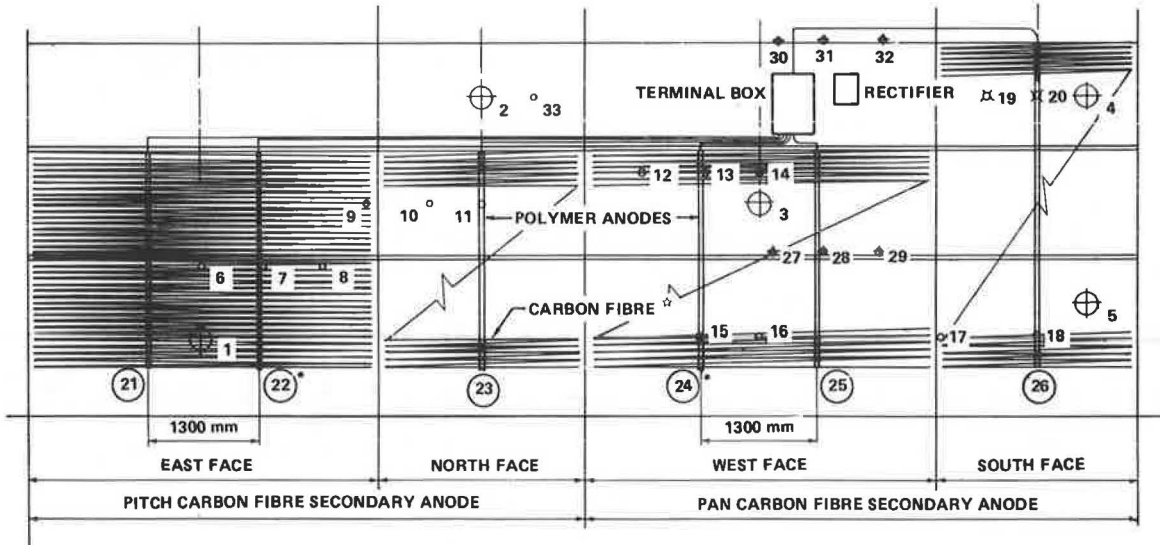
FIGURE 1 System 1: anode and instrumentation placement.



INSTRUMENTATION	1 – 5	MACROCELLS
	6 – 16	CURRENT PICKUP PROBES
	17, 18	CURRENT DISTRIBUTION PROBES
	19 – 22	ANODE LINES
	23 – 25	ELECTRICAL RESISTANCE PROBES

* ANODES DISCONNECTED APRIL 13 - MAY 31

FIGURE 2 System 2: anode and instrumentation placement.



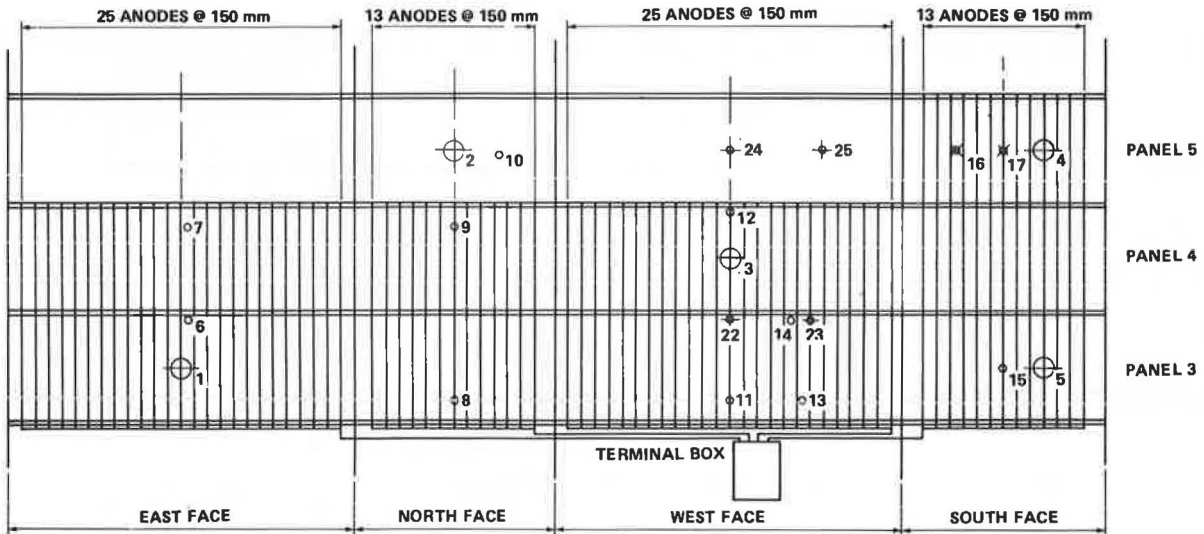
INSTRUMENTATION

- 1 – 5 MACROCELLS
- 6 – 18, 33 CURRENT PICKUP PROBES
- 19, 20 CURRENT DISTRIBUTION PROBES
- 21 – 26 ANODE LINES
- 27 – 32 ELECTRICAL RESISTANCE PROBES

* ANODES DISCONNECTED APRIL 13 - JUNE 6

☆ CARBON FIBRE APPLIED TO ALL FACES AS SHOWN FOR EAST FACE

FIGURE 3 System 3: anode and instrumentation placement.



INSTRUMENTATION

- 1 – 5 MACROCELLS
- 6 – 15 CURRENT PICKUP PROBES
- 16, 17 CURRENT DISTRIBUTION PROBES
- 22 – 25 ELECTRICAL RESISTANCE PROBES

FIGURE 4 System 4: anode and instrumentation placement.

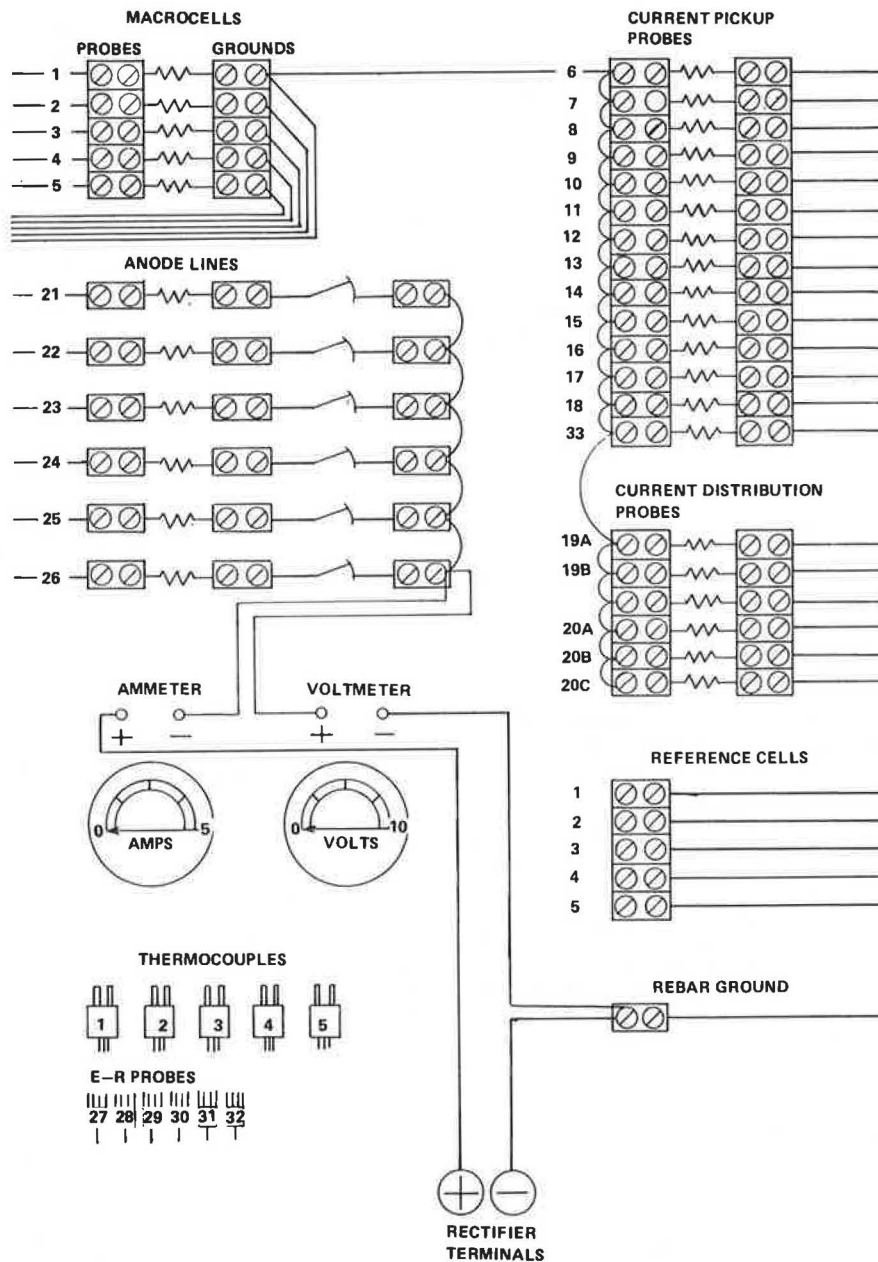


FIGURE 5 Terminal box layout (System 3).

attach the positive lead of the voltmeter to ground. By using this system a positive meter reading indicates the probe is anodic (i.e., corroding). In other words, electron flow is from the probe to the reinforcing steel. Conversely, negative readings indicate that the probe is cathodic (i.e., noncorroding). The readings are expressed in terms of current density on the probe surface in the units $\mu\text{A}/\text{cm}^2$. It is convenient that the numerical value of current density is almost the same in $\mu\text{A}/\text{cm}^2$ and mA/ft^2 (the actual conversion is $1 \mu\text{A}/\text{cm}^2 = 0.93 \text{ mA}/\text{ft}^2$).

Current Pick-Up Probes and Current Distribution Probes

Unlike the macrocell probes, the current pick-up and distribution probes were connected to a common ground. Resistors were placed in each line and the

voltage drop was measured as described in the previous subsection. The magnitude and direction of current flow between each probe and ground was calculated.

Voltage and Potential Measurements

System Voltage

The system voltage in Systems 1, 2, and 3 was measured by connecting a voltmeter across the terminals of the rectifier. In System 4 the instant-off voltages between the anode feeder lines and ground were measured.

Macrocell Reference Cells

The potential of the zinc-zinc sulfate half-cells was measured with respect to the corresponding

macrocell ground. Both a voltmeter and an oscilloscope were used to record on and instant-off cell potentials during the operation of Systems 1, 2, and 3. Potential measurements were also made before activating the systems and during periods of depolarization.

Resistance

The resistance between the anode lines and ground was measured whenever current and voltage measurements were made. A 60-Hz ac resistance meter was used. The electrical resistance probes designed to measure corrosion rates were found to be outside the operating range of the measuring instrument, and no useful data were recorded.

Temperature

The temperature in the concrete at the level of the first layer of reinforcing steel was measured whenever data were collected by using the thermocouples embedded in the macrocells.

PRELIMINARY SYSTEM TESTING

Initial measurements were made before system activation (i.e., no anode-to-ground connections) to ensure that all probes were functioning properly and to obtain system-off unpolarized readings.

E-log I polarization tests were conducted on the four systems to determine the magnitude of corrosion currents in the test columns and to define protection current levels. This test involves application of closely controlled direct current (dc) in a series of increasing increments while monitoring the polarization level of reference cells placed at selected structure points. In this case the anode systems were used to apply the current, and the embedded macrocell reference cells were monitored.

Polarization [instant-off potential (E)] of the cells was plotted against the logarithm of the applied current (log I). The test is described in detail elsewhere (1,2). Tests were conducted as described by Stratfull (1), with minor variations:

1. Current increments, rather than reference cell off potential increments, controlled the progression of the test;
2. Reference cells monitored were not necessarily at the most anodic points of the structure; and
3. Actual current recorded, rather than current density, was plotted.

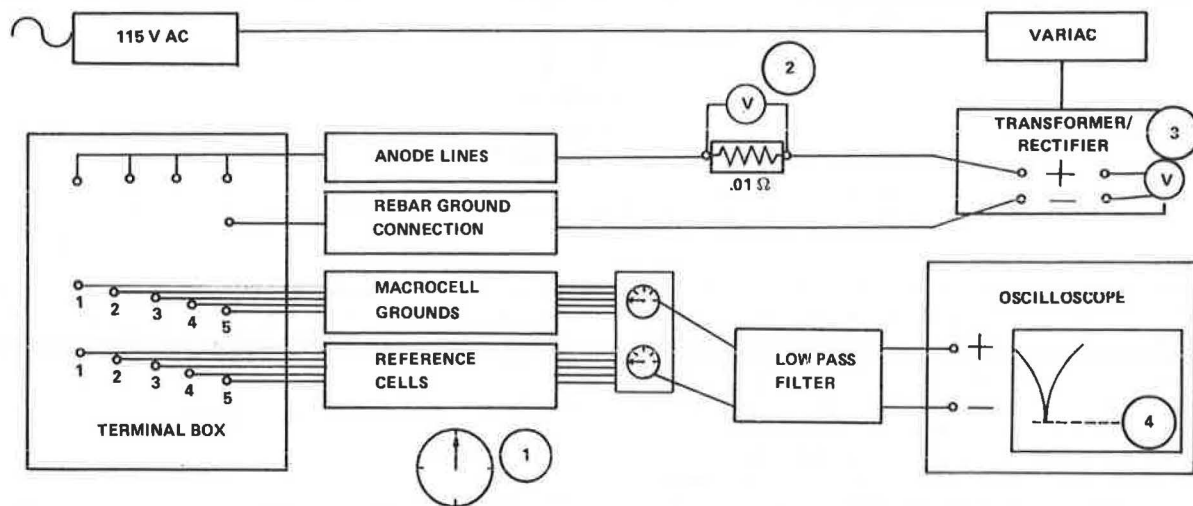
For each test the following parameters were determined:

1. Static half-cell potential for each cell monitored (Estat),
2. Corrosion current (Icorr),
3. Minimum current required for cathodic protection (Icp),
4. Minimum potential required for cathodic protection (Ecp), and
5. Cathodic Tafel slope (8c).

A diagram of the test circuit is shown in Figure 6. A plot prepared from a typical test is shown in Figure 7, with the parameter values labeled.

Initial tests on the three impressed-current systems yielded curves with Icp values ranging from 250 to 780 mA and averaging 418 mA. For purposes of comparison, and to develop data on relative anode consumption rates, all three systems were set at a constant current of 500 mA. This level was maintained throughout the monitoring period described in this paper. System 4 was powered by closing the switches between anodes and corresponding ground leads.

All four systems were activated in November 1982, and monitoring was carried out on a regular basis during the period November 1982 to July 1983. The systems were switched off occasionally and allowed to depolarize so that depolarization rates could be



RECORD DURING TEST

- 1 TIME
- 2 mV DROP (CURRENT = mV DROP/0.01 Ω)
- 3 RECTIFIER OUTPUT VOLTAGE
- 4 REFERENCE CELL "INSTANT-OFF" POTENTIAL - CELLS 1, 2, 3, 4, 5
- 5 VOLTAGE DROPS ACROSS MACROCELL AND CURRENT PICK-UP PROBE RESISTORS (NOT SHOWN)

FIGURE 6 Schematic diagram of instrumentation for E-log I test.

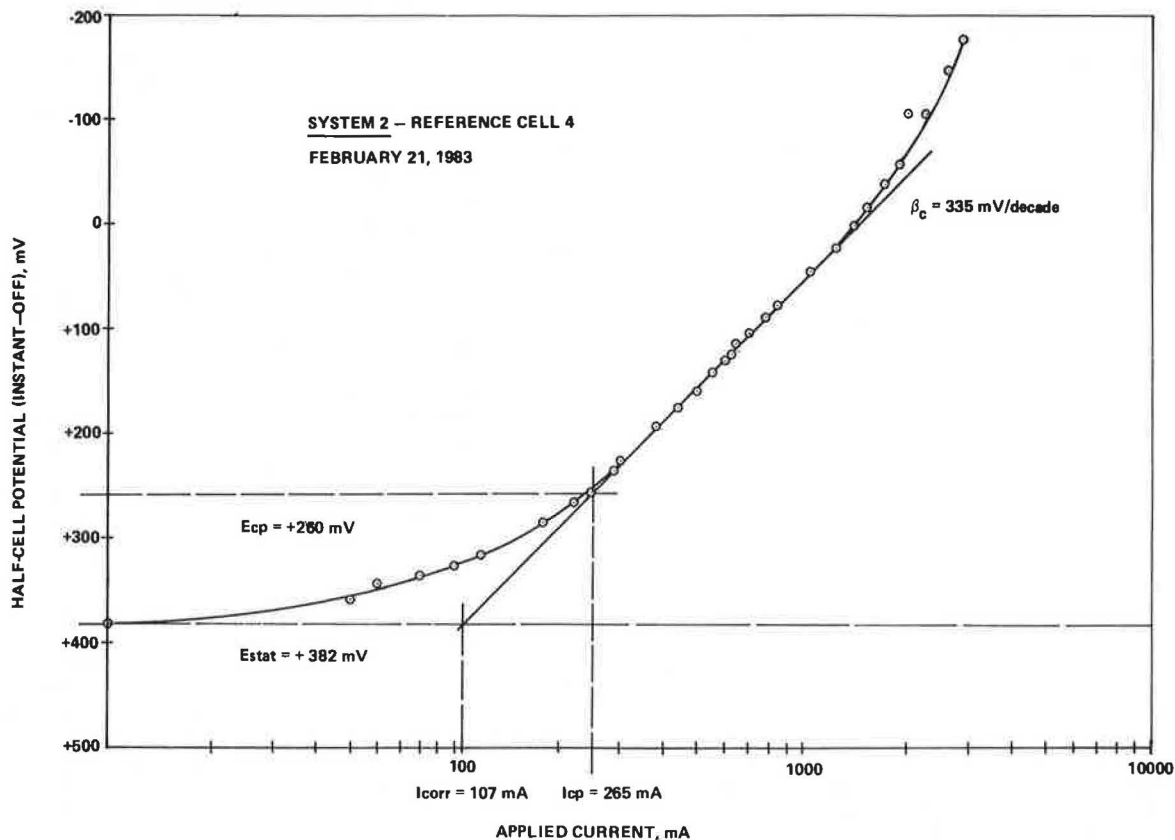


FIGURE 7 E-log I test plot.

monitored and system off conditions examined. E-log I tests were repeated at intervals during these off periods. Later curves yielded values similar to those found in initial tests. As in all E-log I curves, determination of the cathodic Tafel slopes was difficult and subject to interpretation. Additional work is under way to further quantify analysis of these data.

RESULTS OF MONITORING PROGRAM: IMPRESSED-CURRENT SYSTEMS

Current Flow, Density, and Distribution

Anodes and Column Surfaces

A specified applied current of 500 mA resulted in a current density of 13 mA/m² on the protected concrete surface of Systems 1, 2, and 3. The actual current levels were slightly less than 500 mA. The surface area of column reinforcing steel lying beneath the protected portion of each system was estimated to be approximately 17.7 m², which resulted in an average current density on the steel surface of 28.2 mA/m² (2.8 $\mu\text{A}/\text{cm}^2$).

Current densities on the anodes and the separate column faces varied from one system to another because of the different anode configurations. In System 1 there was 5.67 m² primary anode surface. It was initially assumed that all anode surfaces would dissipate current, resulting in a current density of 81 mA/m² of anode surface. Coring has shown that voids exist between the rear anode face and the column concrete, which indicates that the two were not in intimate contact at the time of shotcrete application. Therefore, the three anode faces in

contact with the shotcrete were probably dissipating most of the system current. If this was the case, average current density was increased to 122 mA/m² of anode surface.

In Systems 2 and 3 the presence of a secondary anode increased the effective anode area, thereby lowering current densities in the primary anode systems. In System 2 the conductive paint surface anode covered the entire system area, yielding an overall anode current density of 13 mA/m². In System 3, 20 m of carbon strand anode were used per square meter of concrete surface. Thus each meter of carbon strand, on average, was required to dissipate 0.66 mA of current.

The surface area of the multifilament strand is difficult to calculate, but assuming a diameter of 2 mm for the overbraided pitch fiber yields a calculated current density of 105 mA/m² of fiber surface. Current density on the polyacrylonitrile (PAN) fiber would be somewhat less because of the tendency of this fiber to spread and therefore increase the anode surface area.

Detailed current flow data for the three systems are summarized in Table 1. The values given are the average values during the 8-month period when the systems were operating with all anodes powered. The more significant features of each system are discussed individually.

In System 1 the current densities on the south, east, and west faces were similar. The proportion of current flowing to the north face was less than the other faces because the resistance of the anode line was higher and exhibited greater fluctuations.

In System 2 the resistance of the three anode rings to ground were similar in value but varied over time with fluctuations in temperature and humidity. The percentage of current flowing to each

TABLE 1 Percentage of Total System Current Flowing to Each Anode Line, Corresponding Anode-to-Ground AC Resistance and System Current Densities

System	Anode or Face	Portion of Total Current (%)	AC Resistance (anode to ground) (Ω)	Current Density on Concrete (mA/m^2)
1	North	12.3	26.5	10.4
	South	25.5	16.5	14.3
	East	35.4	11.7	18.3
	West	26.8	15.4	13.9
2	20	34.8	10.4	—
	21	44.6	9.3	—
	22	20.6	11.5	—
3	East face			11.9
	21	6.5	34.3	
	22	17.6	24.1	
	North face: 23	17.0	22.7	14.1
	West face			16.6
	24	20.6	15.7	
	25	11.8	19.6	
	South face: 26	26.5	15.7	14.7
	Pitch anode (north, east)	41.1	—	13.0
	PAN anode (south, west)	58.9	—	15.7

face remained constant. After 7 months of operation the current flowing through anode 20 dropped by considerably more than would be predicted by the change in resistance. The anode will be monitored closely for evidence of deterioration. The current density on each face could not be calculated because the anode system (polymer concrete and paint) is continuous around the column. Anode 19 was installed as shown in Figure 2, but not powered.

The current densities on the four faces of System 3 have remained relatively constant during the monitoring period. However, current flowing to anode 21 has gradually decreased as the resistance has increased.

Macrocells

The five macrocells in each system were placed in the same positions, with one cell outside the protected surface area of each. Before activation of the systems all cells showed positive readings, which indicated anodic current flow on the probe surface. Typical off corrosion current flow to the macrocell probes was on the order of $10 \mu\text{A}/\text{cm}^2$. All probes showed initial fluctuations in current level. In all macrocells within the protected areas of the four systems, current flow between the probe and main reinforcing was reversed by application of a 500 mA cathodic protection current, which indicates that the corroding anodes had been eliminated (i.e., had become cathodes). These cells remained cathodic, when the cathodic protection systems were on, throughout the test period.

Measurements made during E-log I tests indicated that the probes became cathodic at current levels much lower than I_{cp} . Macrocells in all systems outside the protected region showed negligible effects from current application and remained anodic throughout the test period. As the systems were repeatedly polarized and depolarized, macrocell corrosion currents measured during system off periods decreased. However, this effect was also seen on some probes outside protected areas, and thus the reduction in corrosion rate cannot at this time be attributed solely to cathodic protection. Macrocell 3 in System 2 was unstable and showed signs of physical distress. Readings from this cell have therefore been omitted.

Current Pick-Up and Distribution Probes

Average current densities on the probes (including the macrocell rebar probes) have been calculated for the time periods when the systems were activated. The density is calculated by dividing the current flow to or from the probe by the surface area of the probe. These figures are given in Table 2. Values for pick-up and distribution probes when the systems were switched off were essentially zero, showing negligible anodic or cathodic current flow. These off values exhibited no significant variations with time when measured during periods of system depolarization. The probe locations vary from system to system and are shown in Figures 1-4.

The current distribution throughout System 1 was satisfactory, with average probe current densities in the range of 1 to $3 \mu\text{A}/\text{cm}^2$. The distance of the probe from the anode had little effect on the current density received, probably because of the relatively close anode spacing and the presence of the shotcrete overcoat. A slight decrease in current densities was observed as the distance from the power input end of the anodes increased. Probe 9 showed extremely high current densities, although the reason for this is unclear. The probe outside the protected area (in macrocell 2) showed no change when the power was switched on. The average current densities on the distribution probes were 1.93, 0.79, and $0.56 \mu\text{A}/\text{cm}^2$ for probes 100, 180, and 250 mm from the concrete surface, respectively. Thus the probe at the 250-mm depth received 29 percent of the current reaching the probe at the 100-mm depth. A comparison of the average current density on the

TABLE 2 Average Current Densities on Instrumentation Probes

Probe Type and Number	Current Densities ($\mu\text{A}/\text{cm}^2$)		
	System 1	System 2	System 3
Macrocell rebar probes			
1	-4.93	-2.47	-2.42
2	+0.79	+0.47	-2.94
3	-3.24	—	-4.92
4	-2.19	-0.48	-2.93
5	-0.16	-5.09	-1.63
Current pick-up probes			
6	-2.53	-4.26	-4.64
7	-2.34	-0.03	-10.41
8	-2.69	-2.08	-4.12
9	-18.57	-2.22	-1.90
10	-0.67	-3.86	-4.25
11	-1.13	-2.96	-6.55
12	-1.40	—	-4.36
13	-0.53	-2.61	-8.07
14	-3.94	-1.26	-4.61
15	-2.41	-4.95	-8.89
16	—	-11.91	-7.94
17	—	—	-4.75
18	—	—	-6.30
33	—	—	-0.09
Current distribution probes			
16a	-1.41	—	—
16b	-0.74	—	—
16c	-0.66	—	—
17a	-2.61	-1.19	—
17b	-0.84	-1.10	—
17c	-0.51	-0.40	—
18a	-1.79	-3.43	—
18b	-0.53	-1.44	—
18c	-0.49	-0.52	—
19a	-0.24	—	-4.91
19b	-1.04	—	-0.65
19c	-0.59	—	-0.35
20a	—	—	-6.34
20b	—	—	-0.97
20c	—	—	-0.42

distribution probes beneath anodes and remote from the anode lines is shown for all three impressed-current systems in Figure 8.

The current distribution in System 2 was even, with current densities in the range of 2 to 4 $\mu\text{A}/\text{cm}^2$. There was no apparent decrease in protection levels as the distance from the power input end of the anodes increased, which indicates that the paint provided good current distribution. There is no obvious explanation for the abnormally high current level received by probe 16. Probe 7 was located outside the protected area. As with System 1, the current distribution probes showed a significant proportion of the current reaches the 150-mm depth.

The magnitude of current densities measured in System 3 was consistently greater than seen in Systems 1 and 2, generally ranging from 4 to 8 $\mu\text{A}/\text{cm}^2$ for the current pick-up and distribution probes. On all faces the highest current densities were seen directly beneath primary anodes (at probes 7, 11, 13, 15, and 18 the average density was 8.0 $\mu\text{A}/\text{cm}^2$), decreasing midway between anodes (at probes 6, 11, and 16 the average density was 5.7 $\mu\text{A}/\text{cm}^2$), and at a minimum midway between anodes and column edges (at probes 8, 10, 12, and 17 the average density was 4.4 $\mu\text{A}/\text{cm}^2$). However, such a decrease is proba-

bly tolerable. The relationship between the distance of the probe from the primary anode lines and current density is shown in Figure 9. Probe 33, as shown in the figure, is outside the protected area.

Voltage and Potential Measurements

System Voltage

With rectifiers set to maintain a constant current, system voltage levels rise and fall with changes in environmental conditions. Both Systems 1 and 3, with shotcrete overcoats, tended to show stable voltage levels over time with no sudden drops or increases. They showed little variation with short-term temperature changes. System 1 ranged between 3 and 6 V. The lowest voltages occurred during the summer months and the highest voltages occurred during cold winter periods, which corresponds to periods of lower and higher anode-to-ground resistance, respectively. System 3 voltages were in the range of 2.5 to 3.5 V during initial operation, rising to 5 to 7 V during the first winter and remaining near that level (4.5 to 5 V) during the spring and summer of 1983. The ac resistances measured between anodes

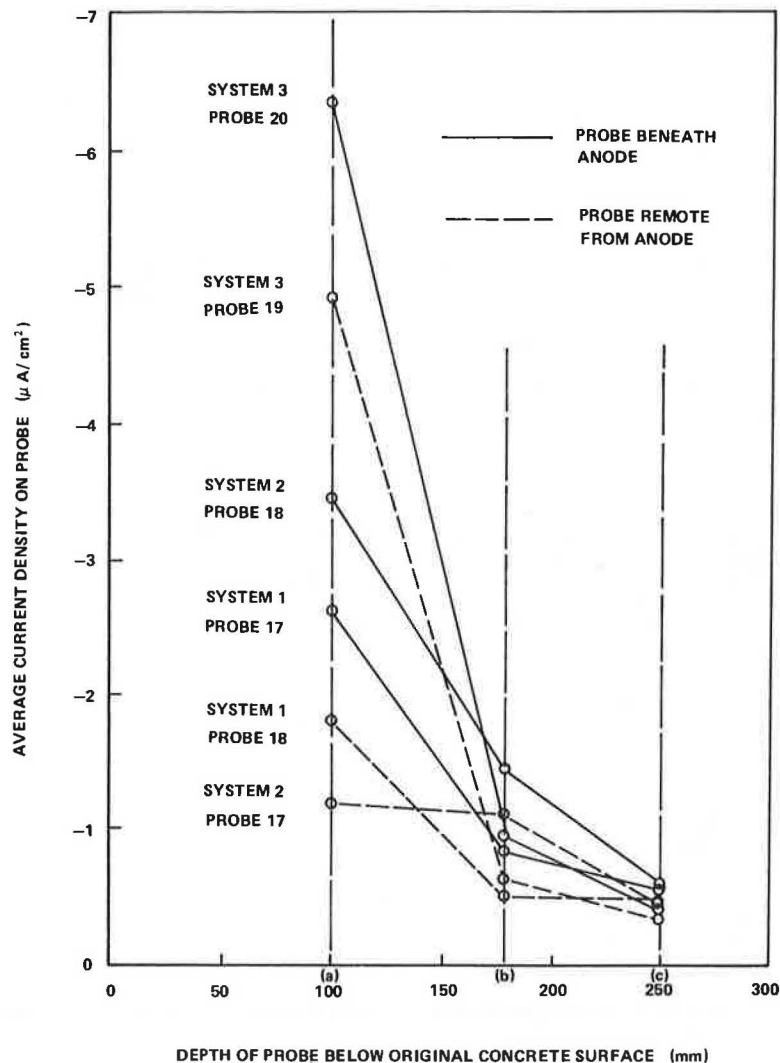


FIGURE 8 Typical variation of average current densities on current pick-up probes with depth and position relative to system primary anodes.

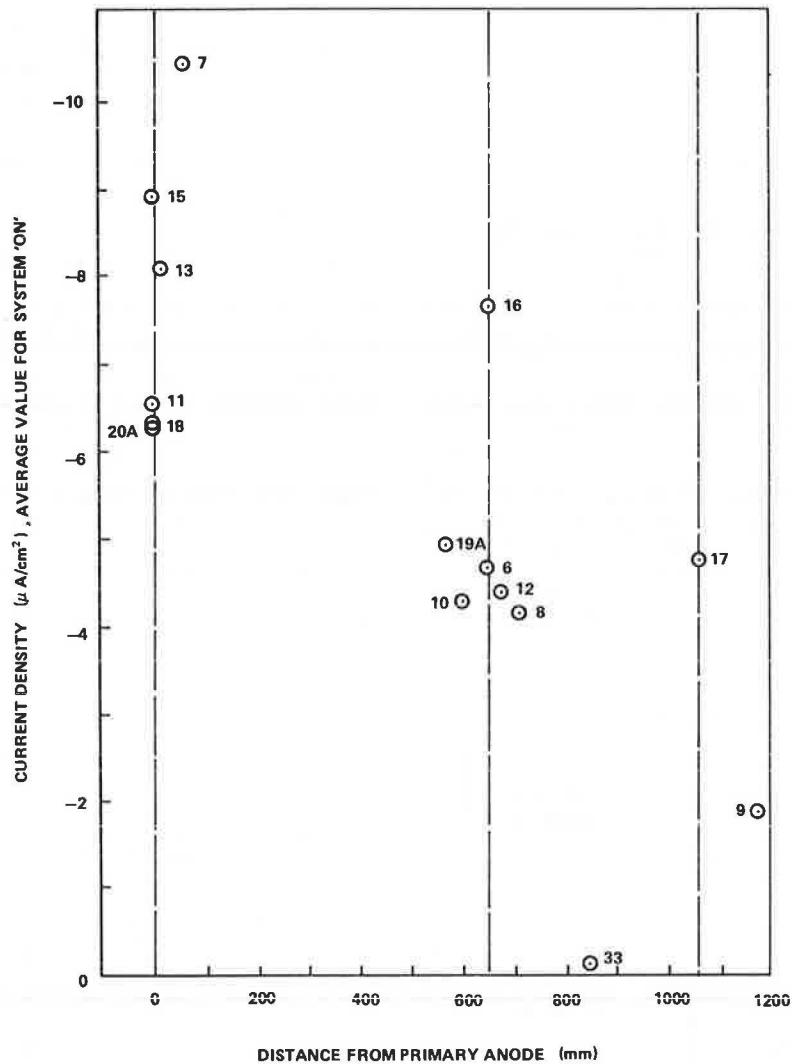


FIGURE 9 System 3: variation of probe current densities with distance of probe from primary anode.

and ground in this system have remained relatively constant. In contrast, System 2 showed rapid and extreme responses to changing temperature and, particularly, humidity conditions. Substantial increases in voltage corresponding to hot dry summer weather occurred and the system was unable to maintain the constant specified current because maximum rectifier output voltage was reached. These high system voltages (13 to 14 V) can be related to increasing anode-to-ground resistance. The resistance readings in July were approximately 4 times those recorded in February. Two factors appear to contribute to this increase in resistance: (a) poor mechanical contact between anode and paint, and (b) drying of the concrete beneath the paint layer.

Examination showed that warping of the anodes between anchoring points had occurred, thus reducing the contact area with the paint. Soaking of the paint on a day when high voltages were recorded caused a drastic drop in voltage, with a threefold increase in system current.

Typical system voltages for the three impressed-current systems are given in Table 3. The dates have been selected to be representative of the conditions experienced during the full 8 months of operation. The temperatures reported are the average concrete

temperatures approximately 100 mm below the original concrete surface.

Reference Cells

Reference cell potentials can be interpreted with

TABLE 3 Typical System Voltages, Selected Dates

Date	Temperature ($^{\circ}\text{C}$)	System Volts		
		System 1	System 2	System 3
November 17, 1982	4.8	4.2	3.6	2.8
November 22, 1982	8.7	4.2	3.0	3.0
January 26, 1983	0.3	5.8	3.9	5.6
March 24, 1983	3.3	5.3	4.3	5.3
April 7, 1983	6.0	6.2	3.1	5.5
April 13, 1983	8.8	4.6	3.8	4.7
April 14, 1983	8.6	6.5 ^a	3.4 ^a	6.4 ^a
April 26, 1983	12.7	6.2 ^a	12.0 ^a	6.6 ^a
June 7, 1983	15.0	6.1 ^a	5.3	5.5
June 16, 1983	27.0	3.2	10.7	5.0
June 21, 1983	26.3	3.3	13.6	5.3
July 8, 1983	24.0	3.3	13.4	4.5

^aAnode arrangement altered.

respect to a number of protection criteria (1,3), including absolute potential values (-850 mV or less with respect to a copper-copper sulfate reference electrode) and potential shifts (-300 mV between static and instant-off potentials, or -100 mV between instant-off potential and steady-state potential of the steel with cathodic protection currents off). Because cell potentials in the test systems varied over a wide range, from cell to cell, while the response of individual cells to current application was generally consistent, a polarization criteria rather than consideration of absolute cell values was most meaningful.

The shift between instant-off potentials and static potential was examined and compared with the specified value of -100 mV. The applied current of 500 mA appears to be more than sufficient to meet this protection criteria for all three systems. The average polarization for the systems over the operating period was -230 mV, based on 10 cells, with cell averages ranging from -187 to -301 mV. The polarization was calculated by subtracting from each instant-off reading the static cell potential measured during the preceding period when the current was switched off. Although static potentials recorded during periods of system depolarization were generally similar, some cells showed a negative shift in static potential with time. This often resulted in a decrease in polarization. For example, the polarization of cell 4 in System 2 decreased from -277 to -134 mV during the monitoring period. This decrease is difficult to interpret. It may be caused by the long-term effects of the application of the cathodic protection, seasonal variations, or changes in the cell itself.

Control cells (cell 2 in all systems) outside the protected area did not all respond the same way and some showed evidence of instability. In System 3 the potential of the cell remained constant, in System 1 the cell showed a steadily increasing negative polarization, and in System 2 cell 2 behaved erratically.

Alteration of Anode Configurations

Some of the anodes were disconnected during the period April to June 1983 to investigate the effects of different anode spacings. In System 1 alternate anodes were disconnected so that the anode spacing was increased to 900 mm. Anode 21 was switched off in System 2 so that the system was powered by two anode rings 2.4 m apart. In System 3 anodes 22 and 24 were switched off so that the east and west faces were powered by a single anode. The maximum distance from a primary anode was then 2.6 m.

The effects of the changed anode spacings were most noticeable in Systems 1 and 3, where the system voltages increased by approximately 30 percent. In System 1 the polarization shift measured by the reference cell directly below an unpowered anode decreased by 50 percent and dropped below 100 mV. Current densities on probes adjacent to unpowered anodes also decreased appreciably in both systems. In System 3 the effect was greater on the east than on the west face, which may indicate less-efficient current distribution on this face. The results indicate that the anode spacings in Systems 1 and 3 cannot be increased significantly unless circuit resistance can be lowered through the use of a more conductive overcoat.

In System 2 there was little change in the potential shift recorded by the reference cells or in the current densities on the pick-up probes, although the current density on two of the macrocell rebar probes decreased. System voltage remained the same

immediately after anode 21 was switched off. It increased later, although this coincided with a period of higher temperature. The test indicated that System 2 distributes current efficiently and primary anode spacing could be increased from 1.2 m to up to 2.4 m.

Effect of Differential Wetting

A short soaking test was carried out on Systems 1 and 2 to determine the effect of wetting part of each system. The south faces of both systems were soaked by hosing for a period of 20 min. The probes were monitored before soaking, 10 min after soaking began, immediately after soaking, and several hours later the same day. A sunny day was chosen so that the temperatures on the south face were high and the concrete surface was dry.

The short soaking period had no effect on any of the current or voltage measurements in System 1. This indicates that the shotcrete insulates the cathodic protection system from sudden environmental changes.

In System 2 the effects of the soaking were immediate. The system voltage required to maintain the 500-mA current dropped from 9.0 to 4.4 V. Reference cells in the the south face showed an average polarization of -135 mV with respect to the initial reading. Cells in the other faces became slightly (40 to 70 mV) more positive. The current flowing to the probes in the wetted face more than doubled, whereas all other probes showed a substantial reduction in current density. The effect of the soaking was reflected in a change in current density on the probes at the 250-mm depth. The change in current distribution in the system was temporary, and within an hour after soaking the readings began shifting to the values observed before soaking. The results illustrate the sensitivity of conductive paint systems to changes in the environment and point to a skin effect (the tendency of the surface concrete to dry), which significantly increases the circuit resistance of paint systems in a dry environment.

Durability

Cores were removed from Systems 1 and 3 after 8 months of operation to examine the anodes and the concrete surrounding the anodes. At the same time, all systems were inspected visually and sounded to detect delamination. This 8-month period represented approximately 2,050 amp-hr of operation for Systems 1 and 3, and 2,270 amp-hr for System 2.

Extensive areas of delamination were found on the north, south, and west faces of System 1, with lesser areas on the east face. The areas of delamination are shown in Figure 10. The delaminations do not correspond to the location of anodes or other physical features. A network of fine cracks was visible in the shotcrete. The cracks were not visible shortly after construction. Cores were taken from the top of an anode on the west face. A strong odor of chlorine gas was evident after the core was removed. The shotcrete was debonded in this area, and a small gap behind the anode indicated it had not been held tightly against the column face during shotcreting. Concrete adjacent to the anode was discolored and deteriorated. Application of pH paper showed acid levels of pH2 on the back of the anode to pH6 on the concrete surrounding the anode. The anode itself showed no deterioration.

In System 2 the paint was found to be adhering well except in areas where new concrete was placed in the macrocells and the rustication strips. The

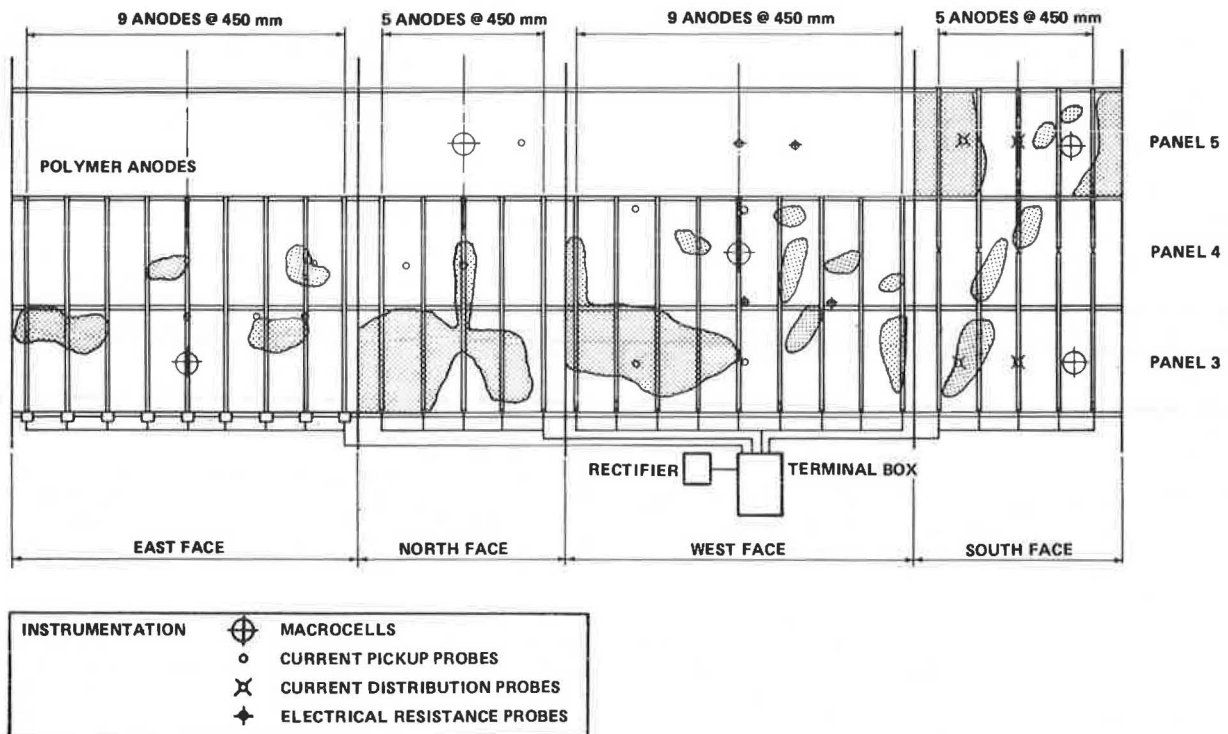


FIGURE 10 System 1: areas of delamination (July 1983).

contact between the anodes and the paint was unsatisfactory, as the anodes had buckled, leaving noticeable gaps between the anodes and the column face. The platinum wire connections appeared brittle and could be easily damaged. There was considerable staining of the paint surface around macrocell 3 by backfill material from the reference cell, which had become unstable. Sounding indicated a small delamination on the top edge of the south face. The shotcrete in System 3 exhibited widespread cracking and extensive delamination in much the same manner as System 1. Coring indicated the delaminations were the result of lack of bond between the shotcrete and the column. The time at which the shotcrete debonded is not known because the shotcrete had not previously been sounded. Cores were also taken about 75 mm from the bottom ends of primary anodes 21 and 22. The core from anode 21 contained cracks that originated from the corners of the anode. The concrete in contact with the anode showed a slight discoloration. Phenolphthalein applied to the core surface

indicated that the concrete adhering to the anode remained alkaline, but the material on the debonded face had a pH less than 9.

The core containing anode 22 also showed that the outer surface of the anode was alkaline while the back face was acidic. Both cores showed the embedded platinum wire and carbon strand to be in excellent condition, and there was firm physical contact between the primary and secondary anodes. The presence of the carbon fiber resulted in a gap between the primary anodes and the concrete surface, and this may have been beneficial in dissipating gases formed on the anode surface.

RESULTS OF MONITORING PROGRAM: SACRIFICIAL ANODE SYSTEM

Current Flow, Density, and Distribution

Anodes and Column Surfaces

The currents and current densities in System 4 were much lower than in the impressed-current systems, typically in the range 1 to 4 mA/m² of concrete surface. The overall current levels fluctuated between a low of 31 mA in April and a high of 141 mA in July, although a slightly higher current was recorded immediately after the system was activated. In general, anode currents were lowest in the winter months. However, currents varied more than would be expected from the changes in anode-to-ground resistance. The resistances showed little consistent seasonal variation but fluctuated considerably from day to day. The distribution of current among the column faces also varied in an unpredictable manner. The data in Table 4 give typical values of current distribution and density throughout the monitoring period. The average current density on the column reinforcing steel during the period was calculated to be 3.7 mA/m² (0.37 μ A/cm²) of rebar surface.

TABLE 4 System 4 Current Distribution

	11/9/82	1/26/83	4/21/83	6/4/83
Temperature ($^{\circ}$ C)	6	-1	6	27
Total current flow (mA)	154	55	56	100
Current flowing to each column face (%)				
North face	24	22	25	16
South face	25	24	23	19
East face	30	36	29	22
West face	21	18	23	43
Current density on column face (mA/m ²)				
North face	6.2	2.0	2.4	2.7
South face	4.3	1.5	1.5	2.1
East face	4.8	2.1	1.7	2.3
West face	3.4	1.0	1.3	4.5

Macrocells

Macrocell current flow was not permanently reversed by the cathodic protection currents. The cells became increasingly positive (i.e., more active) with time, particularly during the summer. The only brief period of current reversal occurred immediately after the system was activated. The behavior of macrocell 4 throughout the monitoring period is shown in Figure 11. By July 1983 all the macrocells were approaching the prepolarization levels of August 1982.

Current Pick-Up and Distribution Probes

The current densities recorded were extremely low, typically $1 \mu\text{A}/\text{cm}^2$ and less for the pick-up probes, and $0.2 \mu\text{A}/\text{cm}^2$ and less for the distribution probes. Slightly higher values were recorded immediately after system activation.

The effect of seasonal variation on the current densities on the pick-up probes is shown in Figure 11. As would be expected, temperature effects were much more significant in System 4 than in the impressed-current systems. There was little difference between the response of the individual probes because of the close (150-mm) spacing of the zinc anodes. Although current was detected on the probes 250 mm below the concrete surface, the levels were extremely low and remained sensibly constant.

Voltage and Potential Measurements

System Voltage

The maximum driving voltage of the system is the potential difference between the zinc and steel, which is theoretically 323 mV. The potential difference measured before coupling the anodes to the reinforcement was approximately 300 mV. The polarized driving voltage during system operation was much lower, typically 70 to 140 mV.

Reference Cells

Before activating the cathodic protection, the potentials of the zinc-zinc sulfate reference cells ranged between +241 and +467 mV. After 8 months of operation the instant-off potentials were between +260 and +338 mV, with an average of +300 mV. Three cells, in macrocells 3, 4, and 5, showed a negative (cathodic) polarization of 70 mV or less based on the difference between the average cell readings before activation and the instant-off potentials after 8 months. Cell 1 showed a slight positive shift. Cell 2, outside the protected region, showed -170 mV (cathodic) polarization. Consequently, in this system the variation of the reference cells with time may mask the true effects of the cathodic protection.

Durability

No cracking or surface damage was observed during the visual examination of the shotcrete in System 4. There was only one small delamination, which was located near the top of the west face adjacent to an unprotected panel.

Cores were taken through an anode on the west face, approximately 150 mm from the anode tip. The appearance of the anode was unchanged from the time of construction and there was no evidence of corrosion of the anode surface. At the time the cores were taken, the quantity of electricity passed was approximately 378 amp-hr. This corresponds to a consumption of 368 g of zinc or 0.50 percent of the total mass of anode.

SUMMARY

All three impressed-current systems were effective from the electrical standpoint of stopping steel corrosion. Operating voltages for the three systems typically lay in the range of 3 to 6 V with systems operating at 500 mA. This resulted in $13 \text{ mA}/\text{m}^2$

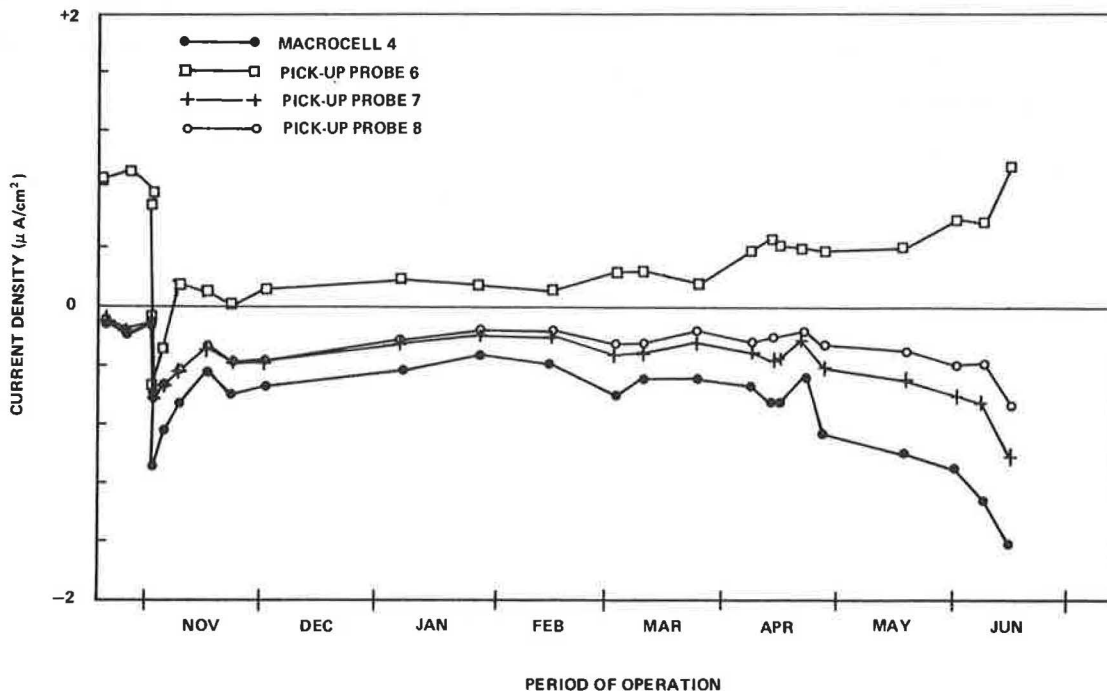


FIGURE 11 System 4: sample macrocell and current pick-up probe current densities during monitoring period.

overall current density on the concrete surface, for all systems, which corresponds to an estimated rebar surface current density of 28.2 mA/m². Pick-up and distribution probe current densities were typically 2 to 6 μ A/cm², with probes at a 250-mm depth receiving significant current. Zinc-zinc sulfate reference cells indicated an average cathodic polarization of approximately 200 mV, with several cells indicating a decrease in rebar polarization as time passed. Three cells showed evidence of instability with time. Probes outside protected areas showed negligible effects due to cathodic protection currents.

Improvements are needed in System 2 where unsatisfactory contact between the primary anodes and the painted concrete surface, coupled with surface drying effects, resulted in high system voltages. The effect of moisture and temperature was much greater in this system than either System 1 or 3. Tests conducted with different anode configurations indicated that the distance between the primary anodes could be doubled to approximately 2.4 m without significantly affecting current distribution.

The anode spacings in Systems 1 and 3 were found to be adequate, but current density calculations and acid attack observed in the core specimens indicated that an increased anode surface will be required. The debonding of the shotcrete has not been adequately explained. The possibility of the cathodic protection currents having an adverse effect requires further investigation, especially in view of results elsewhere with a similar system on a horizontal surface with overlay, which showed no debonding after 18 months at similar anode current densities (4).

The sacrificial anode system offered insufficient protection to the reinforcing steel. Current levels were low, with an average system current of only 65 mA during the 8-month period of evaluation. The system lacked any means of control and exhibited substantial fluctuations in current distribution. The only practical method of increasing current density is to cover the concrete surface with zinc, but a sacrificial system is unlikely to become practicable unless the criteria now assumed to be necessary for adequate protection are found to be unduly conservative.

In all four systems the anode materials showed no degradation after more than 2,000 amp-hr operation on the impressed-current systems and approximately 400 amp-hr on System 4.

All the embedded instrumentation, other than the electrical resistance probes, functioned satisfactorily. The pick-up probes, which were inexpensive

to fabricate and install, were found to be particularly useful in determining the distribution of current over the surface of the reinforcing steel and its variation with depth. The macrocells were useful in determining the effectiveness of the cathodic protection systems. Zinc-zinc sulfate reference cells were found to be unstable, and this simply points to the already well-established need for a reference cell that will be stable when embedded in salt-contaminated concrete.

FUTURE WORK

Although the impressed-current systems stopped corrosion, the durability of the systems must be improved substantially before they would be suitable for a full-scale operational system on bridge substructures. Monitoring of the existing systems will continue and further experimental systems will be constructed at the test site as improved materials are identified. Supporting laboratory and exposure plot studies will concentrate on anode consumption rates, connection details, reference cells, and the effect of cathodic protection on the bond of overcoat materials.

REFERENCES

1. R.F. Stratfull. Criteria for the Cathodic Protection of Bridge Decks. In Corrosion of Reinforcement in Concrete Construction (A.P. Crane, ed.), Society of Chemical Industry, London, England, 1983, pp. 287-332.
2. D. Whiting and D. Stark. Galvanic Cathodic Protection for Reinforced Concrete Bridge Decks: Field Evaluation. NCHRP Report 234. TRB, National Research Council, Washington, D.C., 1981, 63 pp.
3. Recommended Practice: Control of External Corrosion on Underground or Submerged Metallic Piping Systems. Standard RP-01-69. National Association of Corrosion Engineers, Houston, 1972.
4. Y.P. Virmani. FCP Annual Progress Report--Year Ending September 30, 1982, Project 4K, "Cost Effective Rigid Concrete Construction and Rehabilitation in Adverse Environments." FHWA, U.S. Department of Transportation, 1982, p. 40.

Publication of this paper sponsored by Committee on Corrosion and Committee on Performance of Concrete.